

# Polyion–Surfactant Ion Complex Salts Formed by a Random Anionic Copolyacid at Different Molar Ratios of Cationic Surfactant: Phase Behavior with Water and *n*-Alcohols

Ana Maria Percebom,<sup>†</sup> Lennart Piculell,<sup>‡</sup> and Watson Loh\*,<sup>†</sup>

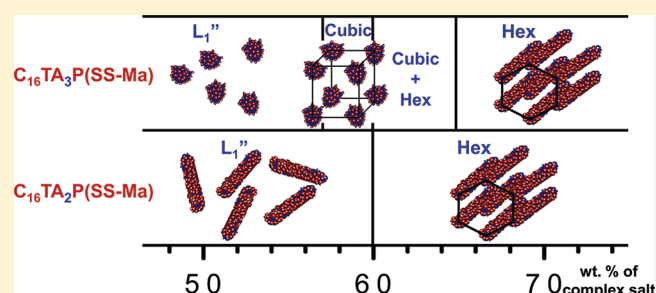
<sup>†</sup>Institute of Chemistry, University of Campinas (UNICAMP), Caixa Postal 6154, Campinas, SP 13083-970, Brazil

<sup>‡</sup>Physical Chemistry 1, Center for Chemistry and Chemical Engineering, Lund University, P.O. Box 124, S-221 00 Lund, Sweden

## S Supporting Information

**ABSTRACT:** The presence of acid groups with different  $pK_a$  values in the anionic copolymer poly(4-styrene sulfonic acid-co-maleic acid), P(SS-Ma), allowed the preparation of complex salts with a variable fraction of anionic groups neutralized by cationic surfactant in the copolymer via controlled titration with hexadecyltrimethylammonium hydroxide,  $C_{16}TAOH$ . Two new complex salts were selected for detailed phase studies,  $C_{16}TA_2P(SS-Ma)$  and  $C_{16}TA_3P(SS-Ma)$ , where both had 100% charged styrene sulfonate groups, but the fraction of charged carboxylate groups on the polyion was 50% or 100%, respectively. These complex salts thus contained both hydrophobic (styrene sulfonate)

and hydrophilic (carboxylate) charged groups, and the ratio between the two could be altered by titration. These features were found to have consequences for the phase behavior in water and in ternary mixtures with water and *n*-alcohols for the two complex salts, which differed compared to complex salts containing homo- or copolyions with only carboxylate or styrene sulfonate charged groups. For both complex salts, binary mixtures with water produced, in the dilute region, two isotropic phases in equilibrium, the bottom (concentrated) one displaying increasing viscosity with increasing concentration. For the complex salt  $C_{16}TA_2P(SS-Ma)$ , there was evidence of micellar growth to form anisometric aggregates at high concentrations. For the  $C_{16}TA_3P(SS-Ma)$  complex salt, this was not observed, and the isotropic phase was followed by a narrow region of cubic phase. In both cases, concentrations above ca. 60 wt % produced a hexagonal phase. For ternary mixtures with *n*-alcohols, the general trend was that a short-chain alcohol such as *n*-butanol acted as a cosolvent dissolving the aggregates, whereas with *n*-decanol, a cosurfactant effect was observed, inducing the formation of lamellar phases. Visual inspection (also between crossed polarizers), small angle X-ray scattering (SAXS) and diffusion nuclear magnetic resonance (NMR) were used in these studies.



## INTRODUCTION

Mixtures of oppositely charged polymers and surfactants in water display associative phase separation as a notable feature.<sup>1</sup> Because of the strong electrostatic attraction, a phase enriched in polyion and ionic surfactant molecules is formed and can exhibit different types of structure (liquid crystalline or disordered micellar systems) making these systems suitable for several applications: as templates, for drug delivery, in cosmetics, and others.<sup>2–4</sup> A considerable number of studies has been developed in order to understand the phase behavior and the interactions involving these species formed by polyions and oppositely charged surfactants. In order to simplify the study of this complex phase behavior, Svensson and co-workers proposed a new strategy,<sup>5</sup> involving the preparation of pure polyion–surfactant ion complex salts (free of simple counterions), which has been applied in several recent studies.<sup>5–19</sup> These studies are important to elucidate how one may control the structure of the (meso)phases formed by these complex salts and their miscibility with water, in terms of the surfactant and polyion features as well as the nature of an added third component.

The focus of the present study is on the consequences of changing the polyion properties. The chemical nature of the charged units of the polyion plays an important role in the involved interactions as verified by Hansson et al.,<sup>20</sup> when comparing complexes formed by sodium polyacrylate, NaPA, and sodium poly 4-styrene sulfonate, NaPSS, with the same cationic surfactant, dodecyltrimethylammonium bromide,  $C_{12}TABr$ . The latter study concluded that the hydrophobic contribution to the interaction between NaPSS and the surfactant is important, whereas for the complex salt formed with polyacrylate, the interaction is essentially electrostatic. Although both polyions are vinyl based, their complexes presented different phase behavior in water, due to the difference in the hydrophobicity of the pendant ionic groups.

In the present work, the random anionic copolymer poly(4-styrene sulfonic-co-maleic acid), P(SS-Ma), containing equal

Received: October 27, 2011

Revised: January 5, 2012

Published: January 30, 2012

amounts of the two acidic monomers, was used to prepare two complex salts to study the combined effect of carboxylate (hydrophilic) and benzenesulfonate (hydrophobic) ionic groups in the same polyion on the complex salt aqueous phase behavior. The present study is also concerned with the effects of varying the fraction of charged carboxylate units neutralized by cationic surfactant molecules along the chain. For this purpose, P(SS-Ma), was titrated with the cationic surfactant hexadecyltrimethylammonium hydroxide,  $C_{16}TAOH$ , to prepare the complex salts  $C_{16}TA_2P(SS-Ma)$  and  $C_{16}TA_3P(SS-Ma)$ . The first possessed surfactant molecules as counterions to all 4-styrene sulfonate groups and half of the carboxylate groups of the maleic acid monomers, the other half remaining as uncharged carboxylic acid groups. In the second complex salt, all titratable groups were charged and neutralized by  $C_{16}TA^+$ . Note that not only the total fraction of charged groups in the two complex salts was different but also the relative proportions of hydrophobic/hydrophilic charged groups.

Previously, Norrman et al. investigated the effect of varying the polyion charge density using  $C_{16}TA^+$  complex salts containing copolyions of acrylate and *uncharged* comonomers in different proportions, namely, poly(acrylate-co-dimethylacrylamide), PA/DAM, and poly(acrylate-co-*N*-isopropylacrylamide), PA/NIPAM, and also partially titrated poly(acrylate/acrylic acid). A decrease in charge density was observed to result in more disordered systems.<sup>8</sup> The  $C_{16}TA_nP(SS-Ma)$  systems studied here can thus be compared with the results of Norman et al. to study the trend of decreasing the polyion charge density.<sup>8</sup> They can also be compared with previously studied systems formed by homopolymers, like  $C_{16}TAPa$ ,<sup>5</sup> and the stoichiometric mixture of  $C_{16}TABr$  and NaPSS,<sup>21</sup> in order to observe the changes when using a polymeric counterion containing ionic comonomers of different chemical nature.

The preparation of pure complex salts (free of simple ions) enabled the direct study of the effect of a third component in mixtures of complex salt and water by determining their ternary phase diagrams. This approach has been previously applied for the addition of organic solvents, surfactants, and polymers.<sup>5,6,9–14</sup> The present work also involved the study of ternary systems containing alcohols with different polarities, *n*-butanol and *n*-decanol, extending the work recently reported by our group.<sup>14</sup>

## EXPERIMENTAL SECTION

**Materials.** Hexadecyltrimethylammonium bromide (99% purity), poly(4-styrene sulfonic acid-co-maleic acid) sodium salt with an average molar mass of  $2 \times 10^4$  g mol<sup>-1</sup> and 1:1 monomer mole ratio and poly(acrylic acid-co-maleic acid) (50 wt % aqueous solution) with an average molar mass of  $3 \times 10^3$  g mol<sup>-1</sup> and 1:1 monomer mole ratio were purchased from Sigma. The alcohols used were *n*-butanol (from Acros) and *n*-decanol (from BDH) of the highest purity available. The deuterated solvents were *n*-butanol-*d*<sub>10</sub> with purity greater than 99.00 atom % *d* obtained from Dr. Glaser A. G. Basel, and deuterium oxide 99.8 atom % *d* from ARMAR Chemicals, Döttingen. Ion exchange resins Dowex Monosphere 550A hydroxide form and Dowex Monosphere 650C hydrogen form were also purchased from Sigma and were activated by stirring in NaOH (1 mol L<sup>-1</sup>) and HCl (1 mol L<sup>-1</sup>), respectively, for one hour, followed by washing with Milli-Q water.

**Syntheses of Complex Salts.** The method developed by Svensson and co-workers<sup>5</sup> was used to prepare the complex salts, with the previous conversion of the anionic copolymer into its acid form by using the acid ion-exchange resin.

Hexadecyltrimethylammonium bromide,  $C_{16}TABr$ , was converted into its hydroxide form,  $C_{16}TAOH$ , by using the basic resin, and the solution obtained was added dropwise to the acid solution of polymer, while the mixture pH was continuously monitored to produce a titration curve. To prepare the complex salt  $C_{16}TA_2P(SS-Ma)$ , the titration was interrupted at the second equivalence point (determined from several titrations to be at pH = 3.0), corresponding to surfactant ions neutralizing half of the carboxylate groups of the maleic acid monomers (after all 4-styrene sulfonate groups have already been neutralized by surfactant ions). The other half remained in the form of uncharged carboxylic acid groups (since such groups are weak acids). In a similar way,  $C_{16}TA_3P(SS-Ma)$  was prepared by interrupting the titration at the third equivalence point (determined to be at pH = 6.0), where all original acid groups were converted to anionic groups (note that the carboxylate ion is a weak base) neutralized by positively charged surfactant ions (Figure 1). No complex salt  $C_{16}TA_1P(SS-Ma)$ , corresponding

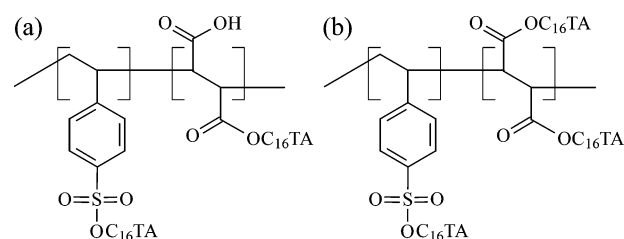


**Figure 1.** Average stoichiometric compositions of the two complex salts: (a)  $C_{16}TA_2P(SS-Ma)$  and (b)  $C_{16}TA_3P(SS-Ma)$ . Note that the copolyion is in reality random but contains an equal fraction of SS and Ma units. The uncharged carboxylic acid groups are free to distribute along the chain.

to a neutralization of only 4-styrene sulfonate groups, was produced, owing to the low pH of the first equivalence point. Such samples would have a very low pH and could possibly degrade during the necessary period for equilibration (at least 1 month).

For comparison, another complex salt,  $C_{16}TA_3P(A-Ma)$ , was prepared in a similar way, through the titration of aqueous poly(acrylic acid-co-maleic acid) with aqueous  $C_{16}TAOH$  up to the last equivalence point (pH = 8.0).

The obtained mixtures of  $C_{16}TA_nP(SS-Ma)$  and water were freeze-dried, and proton nuclear magnetic resonance (<sup>1</sup>H NMR) analyses were performed. Integration of the peaks associated with the methyl protons at the surfactant headgroup, at  $\delta = 3.1$  ppm, and the protons of the copolymer aromatic ring, at  $\delta = 6 - 8$  ppm, confirmed that the stoichiometries between the surfactant and a comonomer pair (SS + Ma) as 2:1 for  $C_{16}TA_2P(SS-Ma)$  and 3:1 for  $C_{16}TA_3P(SS-Ma)$ , with average deviations around 10%.

**Sample Preparation and Analyses.** Samples were prepared immediately after freeze-drying the complex salts to avoid water absorption (the complex salts were relatively hygroscopic). Mixtures of complex salt, water, and when present, alcohol at desired proportions were prepared by weighing each component into glass tubes. The tubes were flame-sealed, mixed with a Vortex vibrator, and centrifuged turning over several times, in order to achieve complete mixing. Later, the samples were left to equilibrate at 25 °C for 30 days, at least, before being analyzed. After visual observation under normal light and between crossed polarizers, the samples could be grouped by features and some were selected to be analyzed by small angle X-ray scattering, SAXS, or nuclear magnetic resonance diffusion measurements.

**SAXS Measurements.** These measurements were performed at the SAXS beamline of the Brazilian Synchrotron Laboratory, LCLS, in Campinas, Brazil. The samples were positioned in a cell with a mica window and temperature control (at 25 °C), the wavelength of X-rays was 1.608 Å, and the sample-to-detector distance was around 0.6 m. The obtained CCD images were integrated and treated with the software Fit2D.<sup>22</sup>

**NMR DOSY Measurements.** Some samples were chosen to be analyzed by NMR diffusion measurements performed at 25 °C on a 200 MHz Bruker DMX spectrometer equipped with a Bruker diffusion probe. To determine the diffusion coefficient of hexadecyltrimethylammonium ions, two pulsed field gradients, PFGs, were applied in the dephasing and refocusing periods of a stimulated echo, STE,  $90^\circ - \tau_1 - 90^\circ - \tau_2 - 90^\circ - \tau_1$  echo. The decays were analyzed with the Stejskal–Tanner expression.

$$I = I_0 \exp[-(\gamma g \delta)^2 (\Delta - \delta/3) D] \quad (1)$$

Here,  $\gamma$  is the magnetogyric ratio of the proton, and  $D$  is the calculated diffusion coefficient. The maximum gradient strength,  $g$ , used was 9.6 T/m, the gradient pulse duration,  $\delta$ , was 0.5 ms, and the diffusion time,  $\Delta$ , was 25 ms. A detailed description of these methods can be found elsewhere.<sup>23–25</sup>

## RESULTS

**Note on Terminology.** The notations used throughout to designate the various disordered or liquid crystalline phases found in this study are explained in Table 1.

**Table 1. Abbreviations of the Various Phases Found in This Work**

term	phase description
$L_1$	water-continuous disordered phase
$L_1'$	dilute $L_1$
$L_1''$	concentrated $L_1$
C	mesophase with cubic structure
H	mesophase with hexagonal structure
L	mesophase with lamellar structure
$L_\alpha$	L without ordering between surfactant chains
$L_\beta$	L with ordering between surfactant chains
$L_2$	alcohol-continuous disordered phase

**Binary Systems (Complex Salt + Water).** The determined binary phase diagrams are presented in Figure 2. Each diagram was based on analyses of around 15 samples. For comparison, a binary phase diagram of the complex  $C_{16}TA_3P$ -(A-Ma) was also determined and is presented in the same figure. At high water contents, both complex salts of  $C_{16}TA_nP$ -(SS-Ma) displayed two isotropic phases: the top phase had low viscosity (dilute- $L_1'$ ) and the bottom phase was highly viscous (concentrated- $L_1''$ ). This phase splitting remained even at very low concentrations (around 0.05 wt % of complex salt), and for this reason, the  $L_1'$  phase region could be assumed to be almost pure water. At intermediate concentrations of complex salts, only the concentrated phase persisted. The transition boundary from the  $L_1' + L_1''$  region to the  $L_1''$  region was determined by the evolution from translucent to clear samples with increasing concentration of complex salt. Translucence in thoroughly mixed macroscopically homogeneous samples was considered to be due to droplets of the dilute phase dispersed

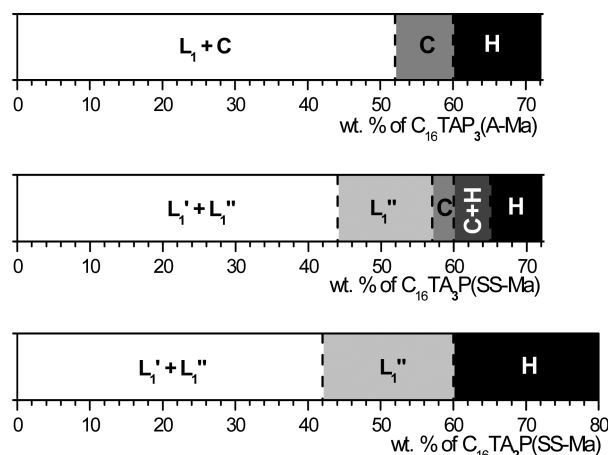


**Figure 2.** Binary phase diagrams of complex salts in water at 25 °C. Dashed lines represent estimated boundaries. From top to bottom, the complex salts are  $C_{16}TA_3P$ -(A-Ma),  $C_{16}TA_3P$ -(SS-Ma), and  $C_{16}TA_2P$ -(SS-Ma).  $L_1'$ , aqueous isotropic dilute phase;  $L_1''$ , aqueous isotropic concentrated phase; C, cubic mesophase; H, hexagonal mesophase.

in the concentrated phase; hence, such samples were considered to belong to the two-phase region. At higher concentrations of complex salts, the mixtures formed liquid crystalline structures that were investigated by SAXS.

In this context, we note that  $C_{16}TA_2P$ -(SS-Ma) is only a quasi-component: it may be regarded as a mixture of, e.g.,  $C_{16}TA_3P$ -(SS-Ma) and the pure acidic polymer. Consequently, in multiphase systems, the proportions of  $C_{16}TA_3P$ -(SS-Ma) and the pure acidic polymer could be different in coexisting phases. In practice, this would only be an issue in wide two-phase areas where both phases contain significant amounts of complex salt. As it turns out, such two-phase areas are rare in the studied  $C_{16}TA_2P$ -(SS-Ma) mixtures here and below. Thus, in Figure 2, the  $L_1'$  phase of the wide  $L_1' - L_1''$  two-phase region is almost pure water, and the two-phase regions at higher concentrations are quite narrow. Consequently,  $C_{16}TA_2P$ -(SS-Ma) will be regarded as one (quasi)component in the following.

The first difference between the two complex salts, observed by the scattering patterns shown in Figure 3, was the formation of a cubic (C) mesophase of the  $Pm3n$  type and of hexagonal (H) structures with the  $C_{16}TA_3P$ -(SS-Ma) system, whereas the system of  $C_{16}TA_2P$ -(SS-Ma) formed only a hexagonal structure (H). Samples with cubic and hexagonal structures were translucent with a pale yellow color, but they could be differentiated because the phase with cubic structure was isotropic and more rigid than the birefringent viscous phase with hexagonal structure.

Also, the  $L_1''$  phases presented evidence of different aggregate shapes for the two complex salts. When  $L_1''$  samples were perturbed by shearing upon mixing, those made from  $C_{16}TA_2P$ -(SS-Ma) became birefringent, whereas the  $C_{16}TA_3P$ -(SS-Ma) samples did not present such an effect. This indicated that the aggregates of  $C_{16}TA_2P$ -(SS-Ma) in the  $L_1''$  phase were anisometric and aligned under flow. This is consistent with the observation that a hexagonal phase, rather than a cubic phase, was the first ordered structure formed by this complex salt at higher concentrations.

The unit cell size,  $a$ , for a sample with cubic structure was calculated by plotting  $(q/2\pi)^2$  as a function of the Miller index according to the following expression:

$$\left(\frac{q_1}{2\pi}\right)^2 = \left(\frac{1}{a}\right)^2 (h^2 + k^2 + l^2) \quad (2)$$



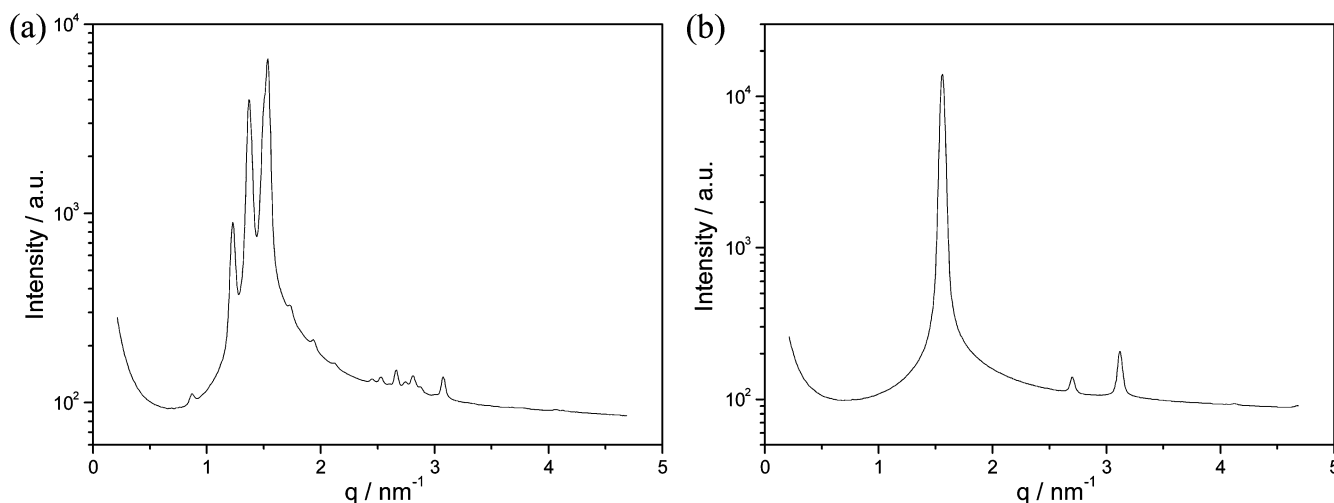


**Figure 3.** SAXS patterns of complex salts in water: (a) cubic + hexagonal phases at 63 wt % of  $C_{16}TA_3P(SS-Ma)$ ; (b) hexagonal phase at 70 wt % of  $C_{16}TA_3P(SS-Ma)$ .

Here, the scattering vector,  $q_1$ , is taken as the position of the first peak.

For the system of  $C_{16}TA_3P(SS-Ma)$ , no sample of single cubic phase was detected because the cubic region was very narrow, but a sample with 63% of  $C_{16}TA_3P(SS-Ma)$  was analyzed by SAXS and presented the spectra of a cubic phase coexisting with a hexagonal phase (Figure 3). As indicated in the diagram presented in Figure 2, the cubic phase was located within the concentration interval of 57–61% of complex salt. This range was used to calculate the aggregation number,  $N_{agg}$ , by dividing the number concentration of surfactant ions (assuming a density of 1 g/cm<sup>3</sup> for the samples) with the number concentration of micelles (assuming 8 micelles per unit cell with a volume of  $a^3$ ). The results are compared in Table 2 with those previously

**Table 2.** Size of Unit Cell,  $a$ , and Aggregation Number,  $N_{agg}$ , for Samples with Cubic Structure of Complex Salts with Different Counterions in Binary Mixtures with Water

sample	$a$ (Å)	$N_{agg}$
$C_{16}TAPA_{30}$ (45 wt %)	101 <sup>a</sup>	100 <sup>a</sup>
$C_{16}TAPMA_{80}$ (45 wt %)	115 <sup>b</sup>	143 <sup>b</sup>
$C_{16}TA_3P(SS-Ma)$ (57–61 wt %)	102	119–128

<sup>a</sup>Reference 9. <sup>b</sup>Reference 12.

obtained for the complex salts  $C_{16}TAPA_{30}$  (with an average of 30 repeating units in the polyacrylate chain)<sup>9</sup> and  $C_{16}TAPMA_{80}$  (hexadecyltrimethylammonium polymethacrylate, PMA, with 80 repeating units).<sup>12</sup>

For hexagonal samples, the radius of the hydrophobic core of the cylindrical aggregate,  $r_{hc}$ , was calculated as

$$r_{hc} = \sqrt{\frac{\phi_{hc} 8\pi}{q_1^2 \sqrt{3}}} \quad (3)$$

using the scattering vector value of the first peak of SAXS spectra,  $q_1$ , and the volume fraction of the hydrocarbon portion of the aggregate,  $\phi_{hc}$ , here assumed to be equal to the sum of volumetric contributions from surfactant alkyl chains. In the calculations, a density of 1 g/cm<sup>3</sup> was assumed both for the hydrophobic core and for the total sample. For more details on the procedure, see ref 6. The calculated radii are presented in

Table 3, where they can be compared with the results for the surfactant  $C_{16}TABr$ <sup>26</sup> and the complex salts  $C_{16}TAPA_{30}$ <sup>9</sup> and  $C_{16}TAPMA_{80}$ .<sup>12</sup>

**Table 3.** Hydrophobic Cylinder Radii ( $r_{hc}$ ) for Samples with Hexagonal Structure of Complex Salts with Different Counter-Polyions in Binary Mixtures with Water

sample	$r_{hc}$ (Å)
$C_{16}TABr$ (47 wt %)	19.6 <sup>a</sup>
$C_{16}TAPA_{30}$ (60 wt %)	16.1 <sup>b</sup>
$C_{16}TAPMA_{80}$ (71 wt %)	17.5 <sup>c</sup>
$C_{16}TA_3P(SS-Ma)$ (70 wt %)	15.7
$C_{16}TA_2P(SS-Ma)$ (77 wt %)	15.1

<sup>a</sup>Reference 26. <sup>b</sup>Reference 9. <sup>c</sup>Reference 12.

### Ternary System (Complex Salt + Water + *n*-Decanol).

For the ternary systems of  $C_{16}TA_2P(SS-Ma)$  and  $C_{16}TA_3P(SS-Ma)$  with water and *n*-decanol, 77 and 36 samples, respectively (numbers depending on the system complexity), were investigated and some (32 and 21, respectively) were selected to be analyzed by SAXS measurements. These data allowed the determination of the ternary diagrams shown in Figure 4.

The addition of even small amounts of *n*-decanol caused the concentrated isotropic phases ( $L_1'$  and cubic), which were present in the binary mixtures, to disappear in favor of a hexagonal- $L_1'$  coexistence. Further addition of *n*-decanol induced the formation of lamellar mesophases ( $L$ ), at intermediary alcohol contents, and of an additional organic isotropic phase ( $L_2$ ), at still higher contents.

The lamellar structures were identified by SAXS analyses (Figure 5), and their samples were viscous (but less so than the hexagonal mesophase), white, and birefringent. For  $C_{16}TA_2P(SS-Ma)$  systems, only one lamellar phase was observed, but for  $C_{16}TA_3P(SS-Ma)$ , the scattering pattern of some samples corresponded to the presence of two lamellar phases. The detection of two coexisting lamellar phases was only possible through SAXS analyses because they have very similar compositions and could neither be separated macroscopically nor distinguished visually. The two phases were tentatively identified as  $L_\alpha$  and  $L_\beta$ , differing in the ordering of the surfactant alkyl chains, based on thorough analyses of previous similar findings for other complex salts in ternary systems with *n*-decanol, namely,  $C_{12}TAPA$ <sup>10</sup> and  $C_{16}TA^+$

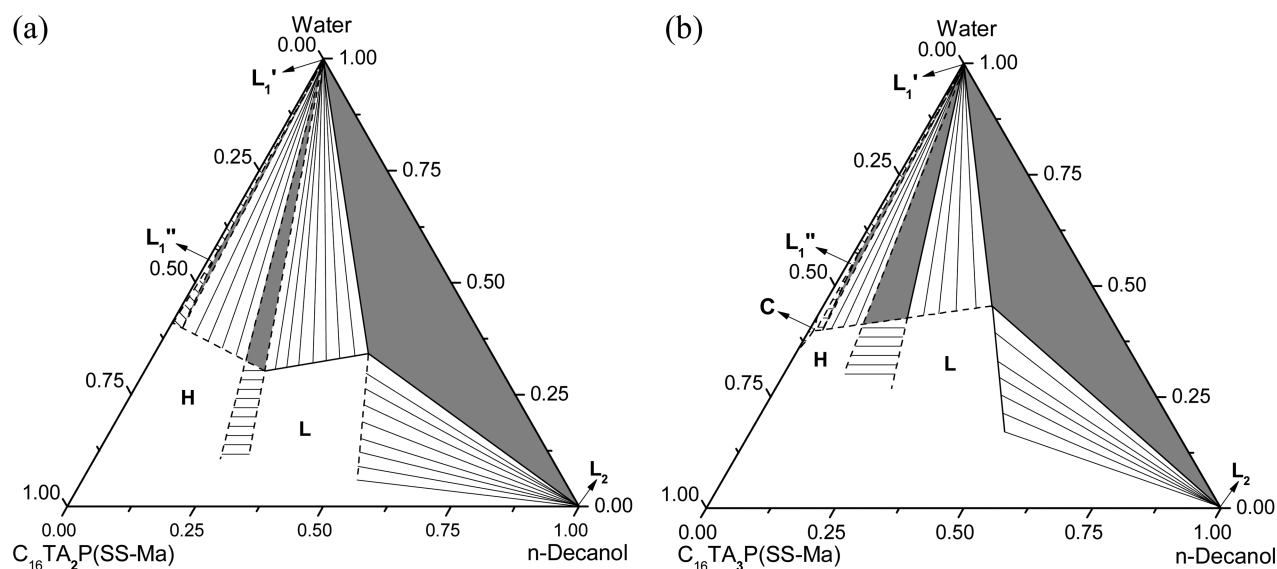


**Figure 4.** Ternary phase diagrams of  $C_{16}TA_nP(SS-Ma)$ /water/ $n$ -decanol at 25 °C. Concentrations are in wt %. (a)  $n = 2$ , (b)  $n = 3$ .  $L_1'$ , dilute aqueous isotropic phase;  $L_1''$ , concentrated aqueous isotropic phase; H, hexagonal mesophase; L, lamellar mesophase;  $L_2$ ,  $n$ -decanolic isotropic phase. Dashed lines represent estimated boundaries, and solid lines represent accurately determined boundaries. White areas represent one-phase regions; areas with a striped pattern represent two-phase regions; gray areas represent three-phase regions.

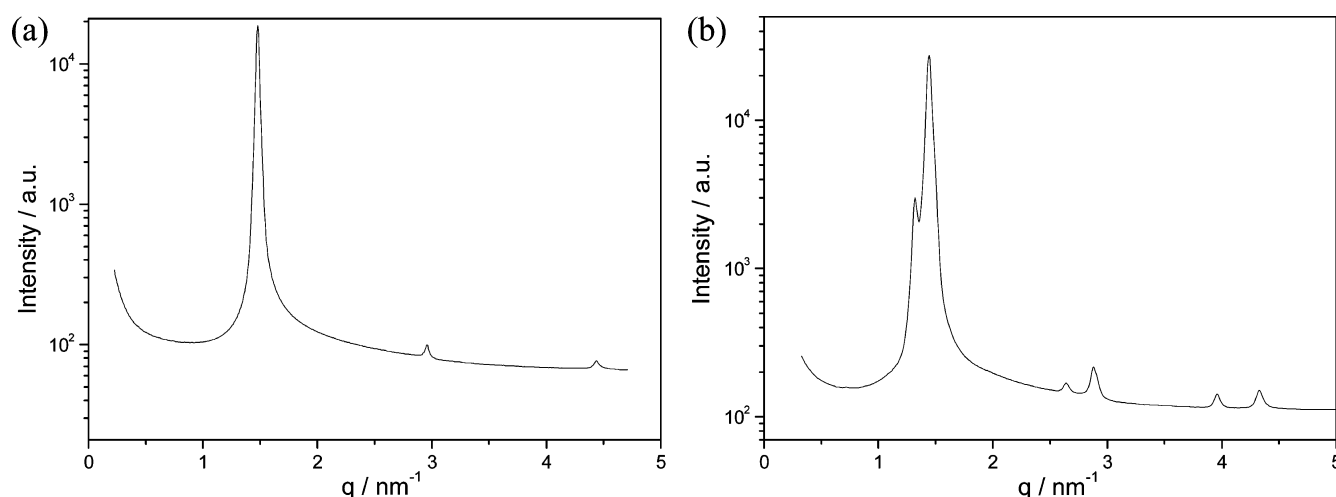


**Figure 5.** SAXS patterns of (a) sample with lamellar structure (37 wt % of  $C_{16}TA_2P(SS-Ma)$ , 23 wt % of water, and 40 wt % of  $n$ -decanol); (b) sample with two coexisting lamellar mesophases (37 wt % of  $C_{16}TA_3P(SS-Ma)$ , 25 wt % of water, and 38 wt % of  $n$ -decanol).

neutralized by oligo carboxylates.<sup>11</sup> X-ray diffraction results for a lamellar sample containing  $C_{16}TA_3P(SS-Ma)$  indeed confirmed (see Figure S3 in the Supporting Information) the presence of a correlation peak corresponding to the distance of 4.2 Å, which is characteristic for the distance between surfactant alkyl chains in the  $L_\beta$  phase.

The isotropic ( $L_2$ ) phase displayed low viscosity, was transparent, and was observed only in coexistence with another phase (at least at concentrations above 0.05 wt % of complex salt), indicating that the  $L_2$  phase was a very dilute system of nearly pure  $n$ -decanol, as a result of the low solubility of complex salt in  $n$ -decanol.

**Ternary System (Complex Salt + Water +  $n$ -Butanol).** Visual analyses of 64 samples of  $C_{16}TA_2P(SS-Ma)$  and 40 of  $C_{16}TA_3P(SS-Ma)$  with water and  $n$ -butanol and SAXS measurements on 29 and 24 selected samples of the respective systems provided the ternary phase diagrams exhibited in Figure 6. Again, the isotropic concentrated phases disappeared with only small amounts of added alcohol. The addition of

more  $n$ -butanol to the  $C_{16}TA_nP(SS-Ma)$  systems leads eventually to a direct transition from the normal hexagonal (H) phase to a reverse micellar system ( $L_2$ ).

The  $C_{16}TA_3P(SS-Ma)$  system showed a significant region of coexistence of hexagonal and  $L_2$  phases, whereas for  $C_{16}TA_2P(SS-Ma)$ , a similar two-phase coexistence was only observed upon slowly heating hexagonal samples with compositions close to the phase boundary. In the latter case, the observation of an  $L_2$  phase coexisting with a hexagonal phase is a strong indication of the absence of lamellar phases in the system.

The  $L_2$  region with  $n$ -butanol was large for both complex salts. The  $L_2$  samples were translucent with a pale yellow color and viscous at higher concentrations of complex salt but became more fluid and transparent upon dilution with  $n$ -butanol. The SAXS spectra of these samples displayed an intense but broad peak indicating that there was a correlation distance between the scattering centers (Figures 7 and 8). The correlation distance,  $d = 2\pi/q$ , for these systems was determined from the position of

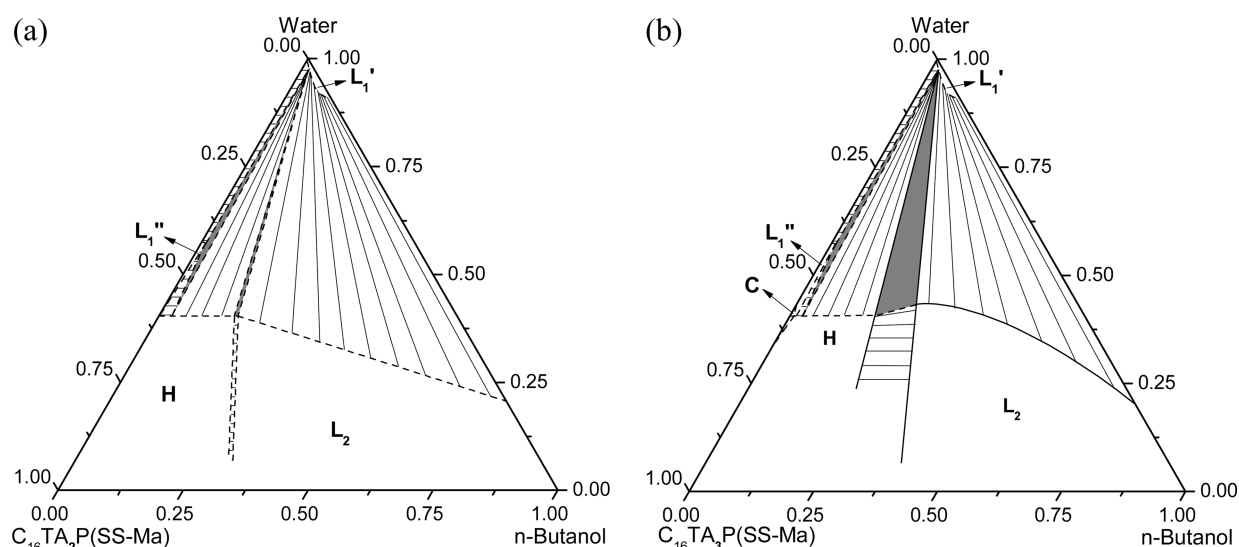


**Figure 6.** Ternary phase diagrams of  $C_{16}TA_nP(SS-Ma)/\text{water}/n\text{-butanol}$  at 25 °C. Concentrations are in wt %. (a)  $n = 2$ , (b)  $n = 3$ .  $L_1'$ , dilute aqueous isotropic phase;  $L_1''$ , concentrated aqueous isotropic phase; H, hexagonal mesophase;  $L_2$ ,  $n$ -butanol isotropic phase. Dashed lines represent estimated boundaries, and solid lines represent accurately determined boundaries. White areas represent one-phase regions; areas with a striped pattern represent two-phase regions; gray areas represent three-phase regions.

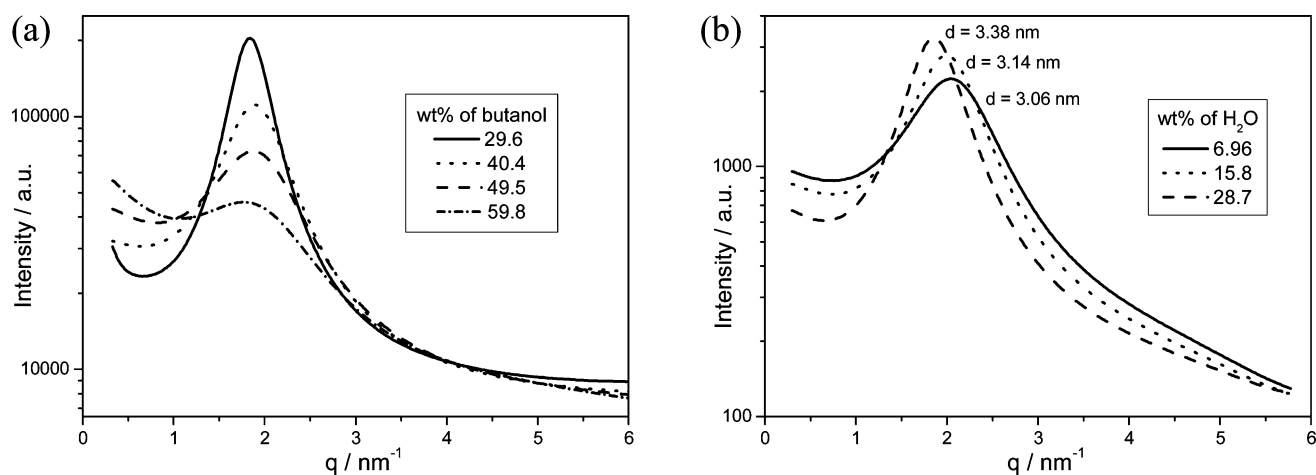


**Figure 7.** Scattering patterns of a series of  $C_{16}TA_2P(SS-Ma)/\text{water}/n\text{-butanol}$  mixtures. (a) Varying the  $n$ -butanol content at a constant complex salt:water mass ratio = 1.4. (b) Varying the water content at a constant complex salt: $n$ -butanol mass ratio = 1.0.

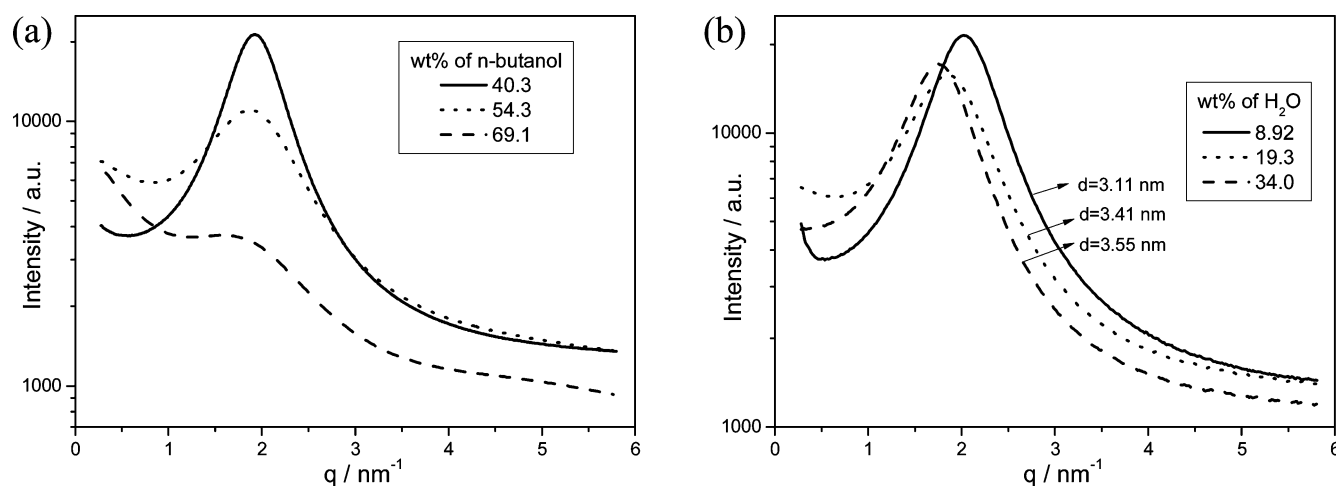


**Figure 8.** Scattering patterns for a series of samples for the systems  $n\text{-butanol}/\text{water}/C_{16}TA_3P(SS-Ma)$ . (a) Varying the  $n$ -butanol content at a constant complex salt:water mass ratio = 1.8. (b) Varying the water content at a constant complex salt: $n$ -butanol mass ratio = 0.57.

the correlation peak,  $q$ , and the obtained values were in the range of 30 to 36 Å.

A previous investigation, using SAXS and diffusion NMR methods, on complex salts of  $C_{16}$ TAPA in *n*-butanol revealed that the  $L_2$  phase consisted of a solution of aggregates where each aggregate was a surfactant-decorated polymer chain with an aqueous core, a so-called reverse micelle with a spine.<sup>13</sup> For the present systems, 10  $L_2$  samples with concentrations varying from 10 to 20 wt % of water and from 0.5 to 2 wt % of complex salt were prepared with deuterated solvents (*n*-butanol- $d_{10}$  and  $D_2O$ ) for NMR measurements of  $C_{16}TA^+$  diffusion coefficients obtained from the signals located at  $\delta = 3.1$  ppm (from the methyl protons at the surfactant headgroup). For the analyzed range of concentrations, the obtained diffusion coefficients varied between  $0.95 \times 10^{-10}$  and  $1.2 \times 10^{-10} \text{ m}^2 \text{ s}^{-1}$  for both complex salts. No significant trend with composition was observed in this small variation. Assuming that the observed value was an average between the diffusion of free surfactant ions, dissociated from the reverse micellar aggregates, and surfactant ions bound to the aggregates, it was possible to calculate the degree of dissociation,  $\alpha$ , using the following relationship:<sup>13</sup>

$$D_{\text{obs}} = \alpha D_{\text{free}} + (1 - \alpha) D_{\text{mic}} \quad (4)$$

Here,  $D_{\text{obs}}$  is the observed diffusion coefficient,  $D_{\text{free}} (= 1.88 \times 10^{-10} \text{ m}^2 \text{ s}^{-1})$ , estimated as described in ref 13) is the free  $CTA^+$  diffusion coefficient in *n*-butanol, and  $D_{\text{mic}} (= 1.42 \times 10^{-11} \text{ m}^2 \text{ s}^{-1})$  is the diffusion coefficient of the micelles. The latter was estimated using the expression appropriate for short rod-like aggregates.<sup>27,28</sup>

$$D = \frac{kT}{3\pi L \eta_0} (\ln(L/d) + \nu) \quad (5)$$

Here,  $L$  and  $d$  are the short rod length and diameter, respectively,  $\eta_0$  is the solvent viscosity, and  $\nu = 0.312 + 0.565/(L/d) - 0.1/(L/d)^2$ . The expression is valid in a regime where  $5 < L/d < 30$ . Assuming that the present systems behave similarly as  $C_{16}$ TAPA systems allowed estimates of the values for  $L$  and  $d$ , respectively, as the length of a fully stretched P(SS-Ma) chain ( $2.9 \times 10^2$  Å) and the cross-sectional diameter of 36 Å, taken from a reverse hexagonal phase of a  $C_{16}$ TAPA complex salt. With these values, and using an *n*-butanol viscosity of 2.62 mPa, one obtains the value of  $D_{\text{mic}}$  given above. The obtained dissociation degrees for the various samples varied between 0.35 and 0.44. The latter values are considerably greater than the value 0.15 obtained for the  $C_{16}$ TAPA complex salt.<sup>13</sup>

## DISCUSSION

**Coexisting Disordered Phases ( $L_1'$  +  $L_1''$ ).** At low concentrations of  $C_{16}TA_nP(\text{SS-Ma})$  in water, there is a segregation of two disordered phases:  $L_1'$  and  $L_1''$ . A coexistence of two disordered phases has previously been observed by Svensson et al.<sup>6</sup> for aqueous complex salts with shorter surfactant chain lengths ( $C_8$ TAPA and  $C_{10}$ TAPA). In the latter systems, the comparatively large maximum water uptake of the concentrated phase, leading to the formation of a disordered micellar solution, was attributed to a large proportion of nonmicellized surfactant ions and a concomitant increased solubility of the complexes. Norrman et al.<sup>8</sup> also observed a disordered concentrated phase for complex salts with copolyions containing uncharged hydrophilic units together with the charged acrylate units. However, in the latter systems, the disappearance of ordered liquid crystalline phases in favor of the disordered phase required a mole fraction of at least 60% uncharged units. By

contrast, for the  $C_{16}TA_nP(\text{SS-Ma})$  systems, concentrated disordered phases coexisting with excess water persist for highly charged polyions, that is, when the polyacids are 67% and 100% neutralized by  $C_{16}TAOH$ .

Comparisons with complex salts of two other polyions put the appearance of a disordered  $L_1''$  phase for the  $C_{16}TA_nP(\text{SS-Ma})$  systems in an interesting perspective. In a stoichiometric mixture of  $C_{16}TABr$  and NaPSS at high water contents, a hexagonal liquid crystalline phase separates out from a dilute aqueous phase.<sup>21</sup> In accordance with the latter observation, mixtures of the complex salt  $C_{16}TAPSS$  with excess water form a hexagonal phase in equilibrium with essentially pure water.<sup>29</sup> Thus, the styrene sulfonate unit per se does not give rise to a disordering of the concentrated phase. However, Figure 2 shows that  $C_{16}TA_3P(\text{A-Ma})$ , based on a copolyion of acrylate and maleate units, features an ordered liquid crystalline phase (in this case cubic, but this may be due to the short length of the copolyion<sup>6</sup>) when swollen in excess water. Taken together, these comparisons indicate that the appearance of a disordered concentrated  $L_1''$  phase for the  $C_{16}TA_nP(\text{SS-Ma})$  systems is due to the simultaneous presence of two very different charged groups in the random copolyion: the carboxylate groups of the maleate units are hydrophilic, whereas the 4-styrene sulfonate group is hydrophobic. NMR chemical shift measurements of aqueous solutions containing  $C_{12}TABr$  and different polyelectrolytes revealed that the aggregate structures are highly influenced by the nature of the polyion.<sup>30</sup> For mixture with NaPSS, the results indicated that the aromatic rings are solubilized in the nonpolar interior of the aggregates, while the sulfonate ion is paired with the surfactant headgroup. We speculate that the random sequence of maleate and styrene sulfonate units in the P(SS-Ma) polyion leads to a variation in the distance-dependent forces between the surfactant aggregates in water-swollen systems, owing to the varying hydrophilic/hydrophobic character of the polyion segments neutralizing the aggregates. This variation might preclude a packing of the aggregates in a regular structure with long-range ordering until, at high concentrations, the aggregate–aggregate interaction potential becomes steeply repulsive. A similar explanation, with locally differing attractive forces between micelles, was invoked to explain the cubic-to-disorder transition that occurs when the acetate counterions of a cubic cetyltrimethylammonium acetate phase are partially replaced by small fractions of short polyacrylate counterions.<sup>9</sup>

**Aggregate Shapes in Binary Mixtures with Water.** The observed shear-induced birefringence indicates the presence of anisometric aggregates, possibly cylindrical, in the concentrated micellar phase,  $L_1''$ , of  $C_{16}TA_2P(\text{SS-Ma})$ . By contrast, the concentrated micellar phase,  $L_1''$ , of  $C_{16}TA_3P(\text{SS-Ma})$  does not present shear birefringence and crystallizes into a cubic structure ( $Pm3n$ ) before forming a hexagonal phase. These observations suggest that the latter complex salt forms aggregates that are closer to spherical. In a similar fashion as described for aqueous solution of NaPSS and  $C_{12}TABr$ ,<sup>30</sup> it can be assumed that, for  $C_{16}TA_2P(\text{SS-Ma})$  in water, the aromatic rings should be at least partially incorporated into the micelle core with the sulfonate close to the surfactant quaternary ammonium groups, hence adding to the hydrophobic core of the micelle and reducing the repulsion between the surfactant polar heads, leading to a decrease in aggregate curvature and an aggregate elongation. Presumably, the presence of a large fraction of uncharged carboxylic acid groups in the copolyion does not prevent such an incorporation of SS units in the



micellar aggregate. However, in the complex salt  $C_{16}TA_3P$ -(SS-Ma), all carboxylate groups are ionic and may pull the polyion chain further out from the micellar surface toward the aqueous domain. Therefore, the aromatic groups no longer reduce the interface curvature to favor a formation of cylindrical aggregates. Note that on the basis of previous studies on polyions containing only carboxylate ionic groups,<sup>8</sup> the increased polyion charge density of  $C_{16}TA_3P$ -(SS-Ma), compared to  $C_{16}TA_2P$ -(SS-Ma), would by itself be predicted to give a *decreased* aggregate curvature, which is opposite to our observations.

**Liquid Crystalline Phases ( $Pm3n$ , Hexagonal, and Lamellar).** Binary mixtures of  $C_{16}TA_3P$ -(SS-Ma) with water feature a cubic structure. The unit cell size and aggregation numbers for the surfactant aggregates formed in cubic phases are presented in Table 2. Bernardes et al.<sup>12</sup> observed that the  $C_{16}TAPMA_{80}$  system presents a larger micellar aggregation number than  $C_{16}TAPA_{30}$ . The aggregation number and unit cell size obtained for  $C_{16}TA_3P$ -(SS-Ma) are similar to the ones observed for the previously studied systems.

The addition of *n*-decanol favors a decrease in aggregate curvature and leads to a transition from the hexagonal phase into a lamellar phase, in agreement with previous findings for complex salts based on polyacrylate<sup>10</sup> and polymethacrylate.<sup>12</sup> However, the estimated maximum molar ratio of *n*-decanol/ $C_{16}TA$  in the hexagonal phase is around 0.74 for ternary mixtures of  $C_{16}TA_2P$ -(SS-Ma), 0.44 for  $C_{16}TA_3P$ -(SS-Ma), 0.32 for complexes with polymethacrylate as counterion,<sup>12</sup> 0.02–0.29 with polyacrylate,<sup>10</sup> 0.16 with sulfate, and 0.04 with bromide.<sup>31</sup> This shows that the hexagonal mesophases formed by  $C_{16}TA_nP$ -(SS-Ma) systems, and especially  $C_{16}TA_3P$ -(SS-Ma), can incorporate a larger amount of *n*-decanol. This may be related to the high aggregate curvature observed for the binary mixtures with water.

For the  $C_{16}TA_3P$ -(SS-Ma) system, the  $L_{\beta}$  phase, which coexists with the  $L_{\alpha}$  one, corresponds to a state in which the chains of surfactant and alcohol molecules are ordered, typically achieved at low temperatures and favored by the addition of long chain *n*-alcohols, also referred to as a gel phase.<sup>11</sup> The observation of a  $L_{\beta}$  phase coexisting with a  $L_{\alpha}$  phase around room temperature has been previously reported for other complex salts with hexadecyltrimethylammonium surfactants, as a result of increased order due to the presence of *n*-alcohols with long alkyl chains.<sup>10,11,32</sup> The previous studies suggest that increasing the amount of *n*-decanol favored the formation of a gel phase, which presented greater distance between the bilayers (lower  $q_1$  value in SAXS spectra) and an extra characteristic distance of 4.2 Å (determined by wide angle X-ray scattering), corresponding to short distance order inside the bilayers, which is the same value obtained in the present study by X-ray diffraction measurement. In the Supporting Information, the area occupied by each hydrocarbon chain (or surfactant and *n*-decanol) and the bilayer thickness in  $L_{\alpha}$  and  $L_{\beta}$  phases, among other structural parameters, are estimated. The obtained values indicate that, due to the ordering between the chains in the lamellar gel phase, the bilayer is thicker and that the area occupied by the hydrocarbon chain is smaller than in the  $L_{\alpha}$  phase. The observed coexistence of the two lamellar phases at room temperature reflects the broad temperature range for the  $L_{\beta}$  to  $L_{\alpha}$  transition, as determined for other complex salts by differential scanning calorimetry.<sup>32</sup> Only one lamellar phase was observed for samples of  $C_{16}TA_2P$ -(SS-Ma) system, that was identified as an  $L_{\alpha}$  phase from the range of  $q_1$  (see Supporting Information).

The maximum amount of water that can be incorporated in the lamellar phases is significantly higher for  $C_{16}TA_3P$ -(SS-Ma) than for  $C_{16}TA_2P$ -(SS-Ma). This trend agrees with the molecular picture proposed above, that the charged carboxylate group in the copolyion is more hydrated than the styrene sulfonate group.

**Reverse Micellar Phase ( $L_2$ ).** The *n*-decanol rich  $L_2$  phase was only observed coexisting with one or two other phases ( $L$  and  $L_1'$ ) indicating that there is a low solubility of  $C_{16}TA_nP$ -(SS-Ma) in *n*-decanol. Because of this low solubility, no investigations by either SAXS or diffusion NMR were conducted on these systems.

When *n*-butanol is added, the concentrated isotropic phases (disordered micellar or cubic) disappear in favor of a hexagonal phase that persists at low and intermediate alcohol contents until the system undergoes a transition into an *n*-butanolic disordered phase ( $L_2$ ) containing aggregates as revealed by the presence of a broad correlation peak in the SAXS patterns (Figures 7 and 8). The correlation distance,  $d$ , calculated from such SAXS results varies little along an *n*-butanol dilution line (adding *n*-butanol at a fixed ratio of complex salt to water). However, with an increase in the water content, there is an increase in the correlation distances. Furthermore, the peaks become broader with *n*-butanol addition and narrower with water addition. This behavior is quite similar to what was previously observed for *n*-alcoholic isotropic phases of  $C_{16}TA$ -PA complex salts.<sup>13</sup> As in the latter system, the  $L_2$  phase for  $C_{16}TA_nP$ -(SS-Ma) in *n*-butanol and water should be composed of an organic continuous medium containing finite reverse micelles, each one formed by one polyion chain dressed with surfactant ions, able to incorporate water molecules in their cores. In the previous work,<sup>13</sup> the observed trends in the SAXS patterns were discussed in detail, using a hexagonal array of rods as a reference model for the local arrangement of the reverse micelles in the  $L_2$  phase. Added water enters both in the micelle core and in the surrounding solvent. In the solvent, water increases the medium dielectric constant, which allows for an increased dissociation of surfactant ions from the reverse micelles. This makes the electrostatic double-layer repulsion between the charged aggregates more important and hence produces more well-defined correlation distances that correspond to thinner peaks. Conversely, with *n*-butanol addition, the correlation distances become less well-defined because the alcohol content increases in the continuous medium. The more or less strong variations in the most probable correlation distance  $d$  with added water or *n*-butanol were tentatively explained as a result of two effects: a trivial dilution effect, and a variation in the degree of stretching of a polyion spine in the reverse micelle.<sup>13</sup>

A direct phase transition from normal hexagonal to reverse micellar phases, as observed in the present diagrams, is unusual because the aggregate curvature normally displays gradual changes. We note that such a direct transition was not observed when *n*-butanol was added to aqueous  $C_{16}TAPA$ ; there, a lamellar phase was found in-between the hexagonal and the reverse micellar phases. Comparing the *n*-butanolic systems for the PA-based complex salts with to the P(SS-Ma)-based complex salts studied here, we find that both the hexagonal phases and the  $L_2$  phases are larger for the latter systems. The increased stability of the hexagonal phase on the addition of *n*-butanol in the P(SS-Ma)-based systems agrees with the pattern seen with added *n*-decanol, described above. The increased extension of the  $L_2$  phase indicates a better solubility in butanol



of reverse  $C_{16}TA_nP(SS-Ma)$  micelles, compared to  $C_{16}TAPA$  reverse micelles. We note that the large degree of dissociation of the surfactant ions from the reverse  $C_{16}TA_nP(SS-Ma)$  micelles, which was inferred from our NMR self-diffusion measurements, should contribute to such a large solubility. It is interesting in this context to note that for mixtures of  $C_{16}TAPA$  with *ethanol*, the normal hexagonal phase is also dissolved directly into an  $L_2$  phase when large amounts of ethanol are added.<sup>14</sup>

## CONCLUSIONS

The present study has demonstrated that a random anionic copolyion, featuring acidic comonomers of different nature (hydrophobic and hydrophilic), offers new possibilities to tune both aggregate shape and aggregate packing in aqueous polyion-surfactant complex salts and their mixtures with alcohols. The simultaneous presence of hydrophobic and hydrophilic units in random sequences in the same polyion prevents the formation of ordered liquid crystalline structures in maximally swollen phases in equilibrium with excess water; instead, disordered micellar phases are formed. Our results support previous findings that the aromatic rings of the styrene sulfonate groups are partially incorporated into the micellar core of the surfactant aggregates, allowing for one-dimensional growth of the aggregates. Interestingly, the partial incorporation of the polyion can be counteracted by introducing charged carboxylate groups on the polyion, and this effect can easily be varied by a simple titration. This gives a possibility to change the shape of the surfactant aggregates, with consequences both for the rheology of the concentrated disordered phase and the preferred structure of the ordered liquid crystalline phase that forms at higher concentrations.

Although their mixtures with alcohols share many of the features previously observed for analogous complex salts based on PA or PMA, important differences were here established for complex salts based on P(SS-Ma). For the latter, the hexagonal phase can incorporate more alcohol, and the disordered  $L_2$  phase in mixtures with *n*-butanol is larger. Again, the detailed features of the complex salt can be tuned by varying the fraction of charged carboxylate units. For the lamellar phase, in particular, 100% charged carboxylate groups leads to the appearance of an  $L_\beta$  phase and to a larger maximum swelling in water.

## ASSOCIATED CONTENT

### Supporting Information

Ternary phase diagrams indicating the compositions of all prepared and analyzed by SAXS samples; the respective results and calculated structural parameters. This material is available free of charge via the Internet at <http://pubs.acs.org>.

## AUTHOR INFORMATION

### Corresponding Author

\*Phone: + 55 19 3521 3148. Fax: + 55 19 3521 3023. E-mail: [wloh@iqm.unicamp.br](mailto:wloh@iqm.unicamp.br).

## ACKNOWLEDGMENTS

Brazilian Agencies FAPESP and CNPq are gratefully acknowledged for the Ph.D. scholarship to A.M.P. and for a senior researcher grant to W.L., respectively. We thank the Brazilian Synchrotron Laboratory, LNLS, for support and the use of the SAXS beamline. We are grateful to Agnieszka Nowacka for her help with the NMR diffusion measurements.

## REFERENCES

- (1) Thalberg, K.; Lindman, B.; Karlström, G. *J. Phys. Chem.* **1990**, *94*, 4289–4295.
- (2) Faul, C. F. J.; Antonietti, M. *Adv. Mater.* **2003**, *15*, 673–683.
- (3) Bronich, T. K.; Nehls, A.; Eisenberg, A.; Kabanov, V. A.; Kabanov, A. V. *Colloids Surf., B* **1999**, *16*, 243–251.
- (4) Hössel, P.; Dieing, R.; Nörenberg, R.; Pfau, A.; Sander, R. *Int. J. Cosmet. Sci.* **2000**, *22*, 1–10.
- (5) Svensson, A.; Piculell, L.; Cabane, B.; Ilekli, P. *J. Phys. Chem. B* **2002**, *106*, 1013–1018.
- (6) Svensson, A.; Norrman, J.; Piculell, L. *J. Phys. Chem. B* **2006**, *110*, 10332–10340.
- (7) Svensson, A.; Topgaard, D.; Piculell, L.; Söderman, O. *J. Phys. Chem. B* **2003**, *107*, 13241–13250.
- (8) Norrman, J.; Lynch, I.; Piculell, L. *J. Phys. Chem. B* **2007**, *111*, 8402–8410.
- (9) Svensson, A.; Piculell, L.; Karlsson, L.; Cabane, B.; Jönsson, B. *J. Phys. Chem. B* **2003**, *107*, 8119–8130.
- (10) Bernardes, J. S.; Norrman, J.; Piculell, L.; Loh, W. *J. Phys. Chem. B* **2006**, *110*, 23433–23442.
- (11) Norrman, J.; Piculell, L. *J. Phys. Chem. B* **2007**, *111*, 13364–13370.
- (12) Bernardes, J. S.; Loh, W. *J. Colloid Interface Sci.* **2008**, *318*, 411–420.
- (13) Bernardes, J. S.; Silva, M. A.; Piculell, L.; Loh, W. *Soft Matter* **2010**, *6*, 144–153.
- (14) Bernardes, J. S.; Piculell, L.; Loh, W. *J. Phys. Chem. B* **2011**, *115*, 9050–9058.
- (15) Piculell, L.; Svensson, A.; Norrman, J.; Bernardes, J. S.; Karlsson, L.; Loh, W. *Pure Appl. Chem.* **2007**, *79*, 1419–1434.
- (16) Piculell, L.; Norrman, J.; Svensson, A. V.; Lynch, I.; Bernardes, J. S.; Loh, W. *Adv. Colloid Interface Sci.* **2009**, *147*, 228–236.
- (17) Santos, S.; Gustavsson, C.; Gudmundsson, C.; Linse, P.; Piculell, L. *Langmuir* **2011**, *27*, 592–603.
- (18) Janiak, J.; Piculell, L.; Olofsson, G.; Schillén, K. *Phys. Chem. Chem. Phys.* **2011**, *13*, 3126–3138.
- (19) Santos, S.; Piculell, L.; Karlsson, O. J.; Miguel, M. G. *Soft Matter* **2011**, *7*, 1830–1839.
- (20) Hansson, P.; Almgren, M. *Langmuir* **1994**, *10*, 2115–2124.
- (21) Zhou, S.; Yeh, F.; Burger, C.; Chu, B. *J. Phys. Chem. B* **1999**, *103*, 21072112.
- (22) Hammersley, A. *FIT2D: An Introduction and Overview*; European Synchrotron Radiation Facility Internal Report, 1997.
- (23) Tanner, J. E. *J. Chem. Phys.* **1970**, *52*, 2523–2526.
- (24) Price, W. S. *NMR Studies of Translational Motion: Principles and Applications*, 1st ed.; Cambridge University Press: Cambridge, U.K., 2009.
- (25) Kimmich, R. *NMR: Tomography, Diffusometry, Relaxometry*, 1st ed.; Springer-Verlag: Berlin, Germany, 1997; Vol. 432.
- (26) Swanson-Vethamuthu, M.; Almgren, M.; Karlsson, G.; Bahadur, P. *Langmuir* **1996**, *12*, 2173–2185.
- (27) Tirado, M. M.; García de la Torre, J. *J. Chem. Phys.* **1979**, *71*, 2581–2587.
- (28) Tirado, M. M.; García de la Torre, J. *J. Chem. Phys.* **1980**, *73*, 1986–1993.
- (29) Kogej, K. Faculty of Chemistry and Chemical Technology, University of Ljubljana. Personal communication.
- (30) Gao, Z.; Kwak, J. C. T.; Wasylshen, R. E. *J. Colloid Interface Sci.* **1988**, *126*, 371–376.
- (31) Fontell, K.; Khan, A.; Lindström, B.; Maciejewska, D.; Puang-Ngern, S. *Colloid Polym. Sci.* **1991**, *269*, 727–742.
- (32) Bernardes, J. S. *Equilíbrio de Fases e Caracterização Estrutural de Sistemas Contendo Poliânions e Surfatantes Catiônicos*. Ph.D. Thesis, University of Campinas, 2008.